Published in final edited form as:
J Heart Lung Transplant. 2012 January ; 31(1): 101–105. doi:10.1016/j.healun.2011.08.022.

A NOVEL WEARABLE PUMP-LUNG DEVICE: IN-VITRO AND ACUTE IN-VIVO STUDY

Tao Zhang, PhD[*], **Xufeng Wei, MD, PhD**[*], **Giacomo Bianchi, MD**[*], **Philip M. Wong, MS**[†], **Brian Biancucci, MS**[†], **Bartley P. Griffith, MD**[*], and **Zhongjun J. Wu, PhD**[*]

[*]Artificial Organs Laboratory, Department of Surgery, University of Maryland School of Medicine, Baltimore, MD 21201, USA

[†]MC3, Inc., Ann Arbor, MI 48103, USA

Abstract

Background—To provide long-term ambulatory cardiopulmonary and respiratory support for adult patients, a novel wearable artificial pump-lung device has been developed. The design features, in-vitro and acute in-vivo performance of this device are reported in this paper.

Methods—This device features a uniquely designed hollow fiber membrane bundle integrated with a magnetically levitated impeller together to form one ultra-compact pump-lung device, which can be placed like current paracorporeal ventricular assist devices to allow ambulatory support. The device is 117 mm in length and 89 mm in diameter and has a priming volume of 115 ml. In-vitro hydrodynamic, gas transfer and biocompatibility experiments were carried out in mock flow loops using ovine blood. Acute in-vivo characterization was conducted in ovine by surgically implanting the device between right atrium and pulmonary artery.

Results—The in-vitro results showed that the device with a membrane surface area of 0.8 m^2 was capable of pumping blood from 1 to 4 L/min against a wide range of pressures and transferring oxygen at a rate of up to 180 ml/min at a blood flow of 3.5 L/min. Standard hemolysis tests demonstrated low hemolysis at the targeted operating condition. The acute in-vivo results also confirmed that the device can provide sufficient oxygen transfer with excellent biocompatibility.

Conclusions—Base on the in-vitro and acute in-vivo study, this highly integrated wearable pump-lung device can provide efficient respiratory support with good biocompatibility and it is ready for long-term evaluation.

INTRODUCTION

Lung disease is the third largest cause of death in the U.S[1]. Acute respiratory distress syndrome (ARDS) afflicts approximately 190,000 U.S. patients yearly with mortality of

Address correspondence and reprint request to: Bartley P Griffith, MD, Department of Surgery, University of Maryland, 22 S Greene Street, Room N4W94, Baltimore, MD 21201, USA, Phone: (410) 328-3822, Fax: (410) 328-2750, bgriffith@smail.uamryland.edu; Zhongjun J Wu, PhD, Department of Surgery, University of Maryland, 10 S. Pine Street, MSTF-436, Baltimore, MD 21201, USA, Phone: (410) 706-7715, Fax: (410) 706-0311, zwu@smail.umaryland.edu.

DISCLOSURE STATEMENT
The authors have no conflicts of interest to disclose.

25%-40%[1]. Irreversible and chronic lung disease can only be treated by lung transplantation. Unfortunately, survival rates after lung transplantation are below other solid organs with a half life of only 5.3 years[2]. The performance is also limited by the availability of donor lungs and the lack of bridge to transplantation options. Current techniques to provide respiratory support include mechanical ventilation and extracorporeal membrane oxygenation (ECMO). Mechanical ventilation is effective for short term support but the prolonged use can often cause other lung injuries. Conventional ECMO could be used as a bridge to transplantation, but it is cumbersome, expensive, and has high mortality and morbidity. Recently, some compact ECMO systems combining new blood pumps and new low-resistance oxygenators have been implemented by innovative physicians in clinics and favourable outcomes were reported[3-7].

Inspired by these developments, we envision a paracorporeally placed artificial lung device may impact quality of life for many respiratory failure patients by opening options for more aggressive medical therapies which may extend survival as well. This device might be reasonably introduced clinically as short-term therapy for ARDS and as a temporary bridge to transplantation. For this purpose, a wearable artificial pump-lung (APL) was developed based on an integrated maglev pump-oxygenator (IMPO)[8, 9] which was designed for bed-side applications. The in-vitro and acute in-vivo experimental results of the APL are presented here.

MATERIALS AND METHODS

Features of Wearable APL

The wearable APL is intended to be used as an ambulatory cardiopulmonary or respiratory support device. It is conceived to draw blood from the vein of the patient through a percutaneous cannula or the right atrium through a surgically implanted cannula and to return oxygenated blood to the pulmonary artery or a large artery. The APL can be paracorporeally placed and the whole system, including motor/controller unit and battery, can be wearable to allow the patient to be mobile. The followings design specifications are proposed: (1) blood flow of 3.5 L/min; (2) oxygen delivery rate of 180 ml/min; (3) pressure head of minimum 100 mmHg; (4) minimized surface area for gas exchange; (5) minimal RBC injury/hemolysis and platelet activation; and (6) support duration of up to 30 days and exchangeable.

To meet the above requirements, a very small magnetic levitation/motor system, currently used for the UltraMag® blood pump (Levitronix, LLC, Waltham, MA, USA)[10], was selected to drive the magnetically levitated impeller and a similar flow configuration was adopted from the previously developed bed-side IMPO[8, 9]. The impeller, diffuser, and flow path from the inlet to outlet, all blood contacting surfaces and surface area of the hollow fiber membranes (HFM) were optimized for pumping function, oxygen transfer and biocompatibility using computational fluid dynamics (CFD) based modeling and design analysis[11]. A plasma resistant HFM material (Oxyplus®, Membrana GmbH, Wuppertal, Germany) was used for the long-term durability.

Figure 1(a) shows the cross-sectional view and magnetically levitated impeller of the APL device. Venous blood is drawn into the pump chamber via the center tube. Driven by the magnetically levitated impeller, the blood flows into the diffuser section, where the diffuser blades guide the blood flow toward the HFM bundle and convert velocity into pressure for improved flow dynamics. Then the blood flows across the HFM bundle radially while rotating around the bundle circumferentially. With oxygen supplied to the HFM bundle, the oxygen is transferred from the fiber lumen to the blood while the carbon dioxide is removed from the blood. The oxygenated blood is collected at the space between the HFM bundle

and the center tube and returned back. The sweep gas enters the HFM bundle lumen from the top and exits the device at the bottom via the channels imbedded in the diffuser fins.

The photographs of the APL device and magnetic suspension/motor drive controller unit are shown in Figure 1(b) and 1(c), respectively. The APL device is 117 mm in length and 89 mm in diameter. The priming volume of the device is 115 ml. The combined weight of the APL device and the motor/controller unit is only 0.54 kg. The port located at the upper right side of the outer housing is used to remove the potentially trapped gas bubbles. The total surface area of the HFM bundle is 0.8 m^2 and the porosity is 0.5, defined as the ratio of the actual volume occupied by the blood to the total volume of the bundle. All the housing components of the wearable APL device are made of medical grade polycarbonate by injection molding except the thin bottom housing that sits into the motor cup and is required for the magnetic levitation. This housing is made of biocompatible titanium. The rotor/impeller assembly consists of a permanent ring-shaped magnet enclosed by a thin titanium shell and a polycarbonate impeller bonded on the top of the rotor (Figure 1(a)). In the future production version, the top gas inlet manifold will be made of opaque polycarbonate and the blood sampling ports will be enclosed into the manifold. A comparison between the APL device and the previous IMPO device is shown in Table 1. Note that the total weight of the IMPO device doesn't include controller.

In-vitro Experiment

The prototype of the APL was fabricated and tested in-vitro first. Filtered and heparinized ovine blood collected from a local slaughter house was used as the testing fluid for all of the in-vitro experiments. The in-vitro pumping performance was tested in a mock circulatory flow loop using blood with 36% hematocrit (Hct) at 37 °C. The in-vitro gas transfer performance was evaluated according to the ISO standard 7199[12] and the ratio of the sweep gas flow rate versus blood flow rate was kept at 1. The in-vitro hemolysis test was conducted according to the ASTM standard F1841-97[13]. A detailed description of the in-vitro experiment setup and procedure can be found in the previous experimental study of the IMPO[9].

Acute In-vivo Experiment

Four acute (one 6-hour and three 24-hour) animal studies were conducted in the ovine model to assess in-vivo hemodynamics, gas exchange function, and biocompatibility of the APL device. The device was surgically connected between the right atrium (RA) and pulmonary artery (PA) of adult Dorsett hybrid sheep. During the course of the study, all animals received humane care in accordance with the Guide for Care and Use of Laboratory Animals (NIH publication 86-23, revised 1996). The surgical protocol and animal care were approved by the Institutional Animal Care and Use Committee of the University of Maryland Baltimore.

The sheep was induced with Pentothal, intubated with ET tube and anesthetized using mechanical ventilation with 1-3% isoflurane. A Swan-Ganz catheter was placed in the PA via the right jugular vein to monitor right atrial pressure, central venous pressure (CVP) and pulmonary artery pressure. A left fourth rib interspace thoracotomy was performed to expose the RA and PA. The sheep was then heparinized to achieve an ACT of above 200 seconds. 10 mm Dacron graft attached to the 10mm outflow cannula was anastomosed end-to-side to the distal PA. A 32 Fr inflow cannula was placed in the RA through the right atrial appendage. A transonic flow probe was placed around the outflow cannula to measure the device flow.

Once the above procedure was completed, both the inflow and outflow cannulae were tunneled and exited the skin. For the 6-hour study, a pre-primed device was connected to the inflow and outflow cannulae and de-aired. Then the device was initiated for the 6-hour in-vivo functional and biocompatibility evaluation. Mechanical ventilation and inspired gas content were adjusted to ensure the normal pH and carbon dioxide partial pressure (pCO_2) in the venous blood. The blood pressure rise across the device, the device flow rate, animal arterial and PA pressures were continuously monitored. Blood samples at the inlet and outlet of the APL device were collected every 30 minutes for blood gas analysis (pO_2, O_2 saturation, pCO_2, Hematocrit, etc) and PFH measurement. For the three 24-hour in vivo experiments, the animals were allowed to recover from the surgery. Continuous heparin infusion was used to maintain the ACT between 150 and 180 seconds. The APL device was operated to produce a blood flow targeted at 3 L/min from the RA to PA. A mixture of 95% oxygen with 5% carbon dioxide was used as sweep gas targeted at 1 L/min to maintain the blood pCO_2 at the inlet of the APL device within the physiological range (between 40 and 50 mmHg). Blood samples at the inlet and outlet of the device were collected every two hours for the first 12 hours and every four hours for the last 12 hours for blood gas analysis and PFH measurement.

RESULTS

In-vitro Results

The pumping performance of the wearable APL is shown in Figure 2(a). These curves represent the ability of the device to generate a pressure head against a pressure afterload at a specific flow rate and a specific rotation speed. At 7000 rpm, the device can deliver a blood flow rate of 3.5 L/min at a pressure head close to 100 mmHg. At the same rotational speed, the pressure head decreases as the flow rate increases. This is achieved by reducing the pressure afterload of the flow loop. This is different from the pressure afterload versus flow rate curve where the pressure afterload increases with the flow rate. To match with the higher pressure afterload, the rotational speed of the pump can be increased to generate a higher pressure head.

The gas transfer performance of the device is shown in Figure 2(b). In general, the oxygen transfer rate increases almost linearly with blood flow rate. This is because the blood was near fully oxygen saturated at the device outlet. At the standard blood hematocrit of 36% for the gas transfer testing, the device was capable of delivering an oxygen transfer rate up to 180 ml/min at a blood flow of 3.5 L/min. The carbon dioxide removal increases almost linearly with blood flow rate until it reaches a plateau at 3 L/min. At the same blood flow rate, the in-vitro CO_2 removal is about 50~70% of the O_2 transfer. At 3 L/min, the CO_2 removal is about 100 ml/min, half of the total CO_2 production for average human. To further increase the CO_2 removal, the sweep gas flow rate can be increased.

The in-vitro blood damage tests at three different blood flow rates with the same rotational speed of 7000 rpm were conducted. The normalized index of hemolysis (NIH) was calculated from the plasma free hemoglobin (PFH) measurements of the blood samples[13]. The results showed that the NIH decreases linearly with the increase of blood flow rate. At the targeted flow rate of 3.5 L/min and higher, the NIH values are less than 0.04, which are comparable to the bed-side IMPO device[9]. This indicates that the wearable APL should have excellent hemo-biocompatibility performance under normal operating conditions. The high NIH at 1.5 L/min may be attributed to the longer blood exposure time to higher shear stress and flow interactions at the interface between the impeller blades and diffuser fins at off-design flow conditions.

In-vivo Results

All the acute in-vivo animal experiments are summarized in Table 2. After surgery, all the three 24-hour animals were able to stand up, eat and drink normally. As shown in Figure 3, the whole system is very compact so it can be fixed on the back of the sheep. Since a mixture of 95% oxygen with 5% carbon dioxide was used as sweep gas, the CO_2 removal capability of the APL device could not be reliably evaluated and was not included in the table. For the first 2 animal studies, the blood flow rate was adjusted intentionally to study its correlation with the oxygen transfer rate. For the last 2 animal studies, the flow rate was kept around 3 L/min. The PFH values of all the animal studies were lower than 20 mg/dl (Table 1) and no significant difference was found between the post implantation values and the baseline values. The in-vivo oxygen transfer performance is shown in Figure 4. In spite of varying inlet blood conditions, the oxygen saturation of the blood at the device outlet was always higher than 95%. A linear trend can still be observed between the oxygen transfer rate and the blood flow rate. The highest oxygen transfer rate was 188 ml/min at a blood flow rate of 4 L/min. Necropsy results of the animals exhibited that there were no infarcts in heart, lung and kidney. Examination of the explanted device indicated that there was no thrombus in the fiber bundle and flow-path of the device.

DISCUSSION

Conventional ECMO systems are inadequate due to their size, complexity, risks and complications. These issues can be substantially alleviated by integrating pumping and oxygenation function together into one device. The major advantages of our APL over other integrated pump-oxygenators[14-20] include magnetically levitated impeller, ultra-compact motor/controller, and unique circumferential-radial flow path design. The only moving component is the impeller and no mechanical shaft, bearing or seal is required. Therefore the risks of blood trauma and component failure are greatly reduced. The size and weight of the motor/controller are very small so the patient can walk and practice wearing the whole system. The CFD optimized flow path design ensures the flow fields across the HFM bundle are uniform without stagnation and highly efficient gas transfer can be achieved.

The application of APL could be flexible to match multiple clinical needs. Although only one configuration was tested in-vivo, APL may be used in three configurations: right atrium to pulmonary artery, right atrium to descending aorta, and percutaneous connection. The required pressure head against the afterload for these configurations will vary from 15 mmHg to 100 mmHg and the rotational speed can be adjusted to meet the requirements.

Acknowledgments

This work was supported by the National Institutes of Health (Grant No.: R01HL082631, R42HL084807, and R01HL088100).

REFERENCES

1. American Lung Association. [Accessed on July, 2011] Lung Disease Data. 2008. http://www.lungusa.org/about-us/publications/
2. Christie JD, Edwards LB, Kucheryavaya AY, et al. The Registry of the International Society for Heart and Lung Transplantation: twenty-seventh official adult lung and heart-lung transplant report--2010. J Heart Lung Transplant. 2010; 29(10):1104–18. [PubMed: 20870165]
3. Aziz TA, Singh G, Popjes E, et al. Initial experience with CentriMag extracorporal membrane oxygenation for support of critically ill patients with refractory cardiogenic shock. J Heart Lung Transplant. 2010; 29(1):66–71. [PubMed: 19837609]

4. Camboni D, Philipp A, Haneya A, et al. Serial use of an interventional lung assist device and a ventricular assist device. ASAIO J. 2010; 56(3):270–2. [PubMed: 20335803]
5. Griffith KE, Jenkins E, Haft J. Treatment of massive pulmonary embolism utilizing a multidisciplinary approach: a case study. Perfusion. 2009; 24(3):169–72. [PubMed: 19793777]
6. Russo CF, Cannata A, Lanfranconi M, et al. Veno-arterial extracorporeal membrane oxygenation using Levitronix centrifugal pump as bridge to decision for refractory cardiogenic shock. J Thorac Cardiovasc Surg. 2010; 140(6):1416–21. [PubMed: 20933244]
7. Garcia JP, Iacono A, Kon ZN, Griffith BP. Ambulatory extracorporeal membrane oxygenation: a new approach for bridge-to-lung transplantation. J Thorac Cardiovasc Surg. 2010; 139(6):e137–9. [PubMed: 20219215]
8. Zhang J, Taskin ME, Koert A, et al. Computational design and in vitro characterization of an integrated maglev pump-oxygenator. Artif Organs. 2009; 33(10):805–17. [PubMed: 19681842]
9. Zhang T, Cheng G, Koert A, et al. Functional and biocompatibility performances of an integrated Maglev pump-oxygenator. Artif Organs. 2009; 33(1):36–45. [PubMed: 19178439]
10. Taskin ME, Fraser KH, Zhang T, et al. Computational characterization of flow and hemolytic performance of the UltraMag blood pump for circulatory support. Artif Organs. 2010; 34(12): 1099–113. [PubMed: 20626739]
11. Wu ZJ, Taskin EM, Zhang T, Fraser KH, Griffith BP. Computational Model-Based Design of a Wearable Artificial Pump-Lung for Cardiopulmonary/Respiratory Support. Accepted for publication in Artif Organs.
12. International Organization for Standardization. 1996. ISO 7199: Cardiovascular implants and artificial organs-blood gas exchangers (oxygenators).
13. American Society for Testing and Materials. 1997. ASTM F1841-97: Standard Practice for Assessment of Hemolysis in Continuous Flow Blood Pumps.
14. Wu ZJ, Gartner M, Litwak KN, Griffith BP. Progress toward an ambulatory pump-lung. J Thorac Cardiovasc Surg. 2005; 130(4):973–8. [PubMed: 16214507]
15. Svitek RG, Frankowski BJ, Federspiel WJ. Evaluation of a pumping assist lung that uses a rotating fiber bundle. ASAIO J. 2005; 51(6):773–80. [PubMed: 16340367]
16. Tatsumi E, Takano H, Taenaka Y, et al. Development of an ultracompact integrated heart-lung assist device. Artif Organs. 1999; 23(6):518–23. [PubMed: 10392277]
17. von Segesser LK, Tozzi P, Mallbiabrrena I, Jegger D, Horisberger J, Corno A. Miniaturization in cardiopulmonary bypass. Perfusion. 2003; 18(4):219–24. [PubMed: 14575410]
18. Arens J, Schnoering H, Pfennig M, et al. The Aachen MiniHLM--a miniaturized heart-lung machine for neonates with an integrated rotary blood pump. Artif Organs. 2010; 34(9):707–13. [PubMed: 20883389]
19. Pantalos GM, Horrell T, Merkley T, et al. In vitro characterization and performance testing of the ension pediatric cardiopulmonary assist system. ASAIO J. 2009; 55(3):282–6. [PubMed: 19293710]
20. Kopp R, Bensberg R, Arens J, et al. A miniaturized extracorporeal membrane oxygenator with integrated rotary blood pump: preclinical in vivo testing. ASAIO J. 2011; 57(3):158–63. [PubMed: 21317635]

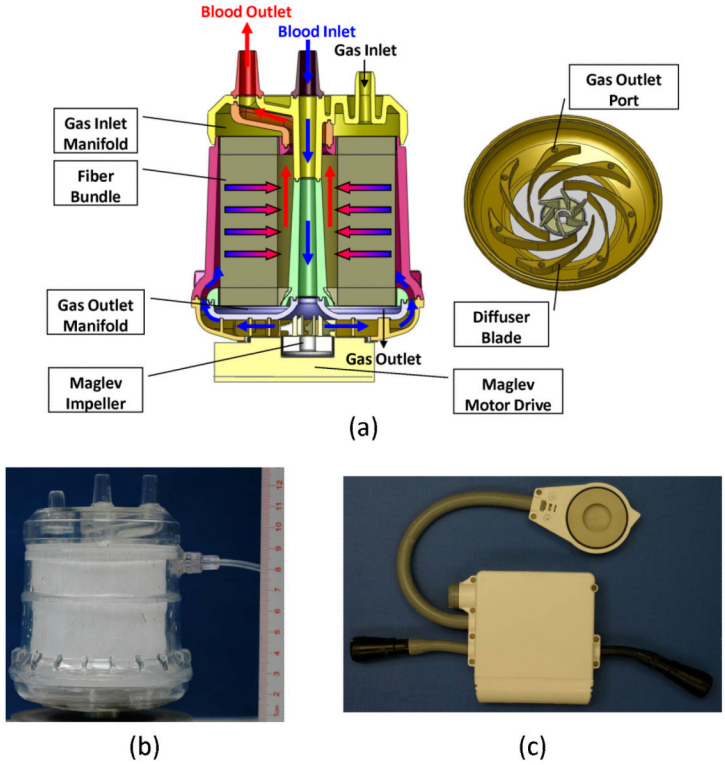

Figure 1.
(a) Drawing of the cross-section and the impeller/diffuser assembly of the APL device; (b) Photo of the device; and (c) Photo of the motor/controller system.

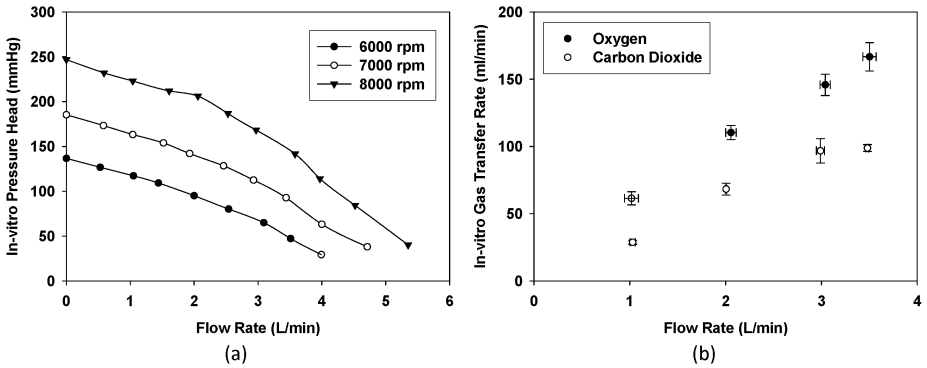

Figure 2.

(a) In-vitro pumping performance of the APL device; and (b) In-vitro gas transfer performance of the APL device (Error bar represents standard deviation.).

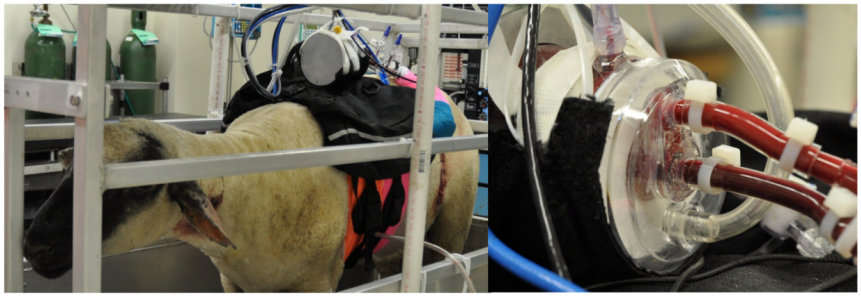

Figure 3.
Photos of the in-vivo animal study: (a) The APL device fixed on the back of the sheep; and (b) Enlarged view of the APL device.

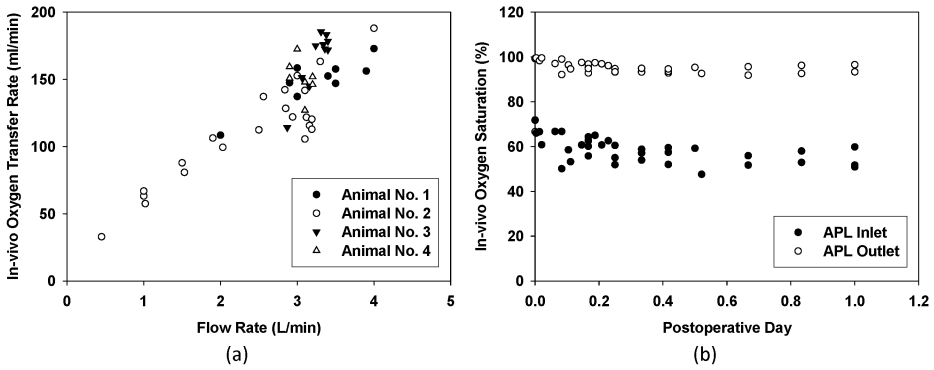

Figure 4.

(a) Oxygen transfer results of the in-vivo studies; and (b) Inlet and outlet oxygen saturation variation during the in-vivo studies.

Table 1

Comparison between APL and IMPO

	IMPO	APL
Diameter (mm)	97	89
Height (mm)	144	117
Surface Area (m^2)	1.05	0.8
Porosity	0.55	0.50
Priming Volume (ml)	200	115
Total Weight (kg)	1.9	0.54
Flow Range (L/min)	1~7	1~4
Fiber Material	Polypropylene	Polymethylpentene
Usage	Bedside	Wearable

Table 2

Summary of the in-vivo animal experiments (PFH data are given as mean ± standard deviation.)

Sheep Number	Weight (kg)	Duration (hour)	Device Flow (L/min)	0_2 Transfer (ml/min)	PFH (mg/dL)	Plasma Leakage
1	50.0	6	1–4	63–173	10.7±3.6	no
2	46.5	24	0.5–4	33–188	7.2±2.6	no
3	50.9	24	2.9–3.4	114–185	12.5±3.3	no
4	53.8	24	2.9–3.2	89–172	13.6±3.6	no